PHYSICAL REVIEW A VOLUME 4, NUMBER 3 SEPTEMBER 1971

Close-Coupling Studies of Rotational Excitation in H-H_2 Collisions

Edward F. Hayes
Department of Chemistry, Rice University, Houston, Texas 77001

and

Charles A. Wells and Donald J. Kouri
Department of Chemistry, University of Houston, Houston, Texas 77004
(Received 15 January 1971)

Close-coupling calculations are reported for low-energy H-H_2 collisions. These results are compared with Tang's distorted-wave calculations of the differential and total cross sections for the $j=0$ to $j=2$ rotational transition. The close-coupling results for the total cross section are found to agree quantitatively with the distorted-wave results. Furthermore, the relative transition probabilities for various partial waves determined by Tang agree qualitatively with the close-coupling results reported here. The strong forward peaking in the cross section $\sigma(\theta)$ reported by Tang is also found in the present study. However, there appear to be significant differences in the magnitudes and positions of oscillations in the differential cross sections as determined by the close-coupling and distorted-wave methods. Finally, close-coupling results for the $j=0$ elastic scattering differential cross section are presented and discussed briefly.

I. INTRODUCTION

Recently distorted-wave studies of rotational excitation of H_2 molecules by collisions with H atoms were reported by Tang.[1] In that paper, a new potential function was employed in an attempt to describe properly the interaction in both the valence and long-range regions. The potential is in the form of a multipole series which was fitted to a semiempirical surface designed to describe the H-H_2 interaction in the region between 1 and 5 bohr.[2] The potential is such that it is possible to join smoothly onto the correct long-range form resulting from the perturbation studies of Dalgarno, Henry, and Roberts.[3] Because of the importance of this system as a prototype for more complex atom-molecule collisions and as an important astrophysical system, it is of interest to make detailed calculations of scattering employing the new potential surface. Furthermore, Tang's distorted-wave results were found to be in rather striking contrast to results obtained from earlier potential functions by Dalgarno, Henry, and Roberts.[3] In particular, strong forward peaking in the differential cross sections was found by Tang at all energies studied, whereas the Dalgarno, Henry, and Roberts study showed very strong dominance of backward scattering. Further, the behavior of the differential cross section at higher energies was not monotonic; rather, one noticed a building up of a backward peak as the energy was increased. Tang interpreted these results in terms of competition between scattering dominated by the attractive and repulsive portions of the potential. Further, the potential Tang used is interesting in that the coefficient of P_2 contains more than one repulsive region. Finally, the differential and total cross sections were roughly an order of magnitude smaller than the Dalgarno, Henry, and Roberts results (the same conclusions held for comparison of Tang's results with close-coupled equation results of Allison and Dalgarno[4]).

Because of the significant qualitative and quantitative differences between the results reported by Tang[1] and those of Dalgarno, Henry, and Roberts,[3] it seems worthwhile to carry out close-coupling calculations to determine how the distorted-wave approximation influenced Tang's results and what features of his results can be attributed to the potential he employed. Section II contains a brief discussion of the method employed for the close-coupling studies and the results of a study of He-H_2. These calculations are presented to support the accuracy of the computer programs used in this study. In Sec. III, a comparison of the close-coupling results is made with those obtained by Tang for the inelastic differential and total cross sections for the $j=0$ to $j=2$ transition. The importance of including a sufficient number of terms in the multipole expansion of the differential cross sections at angles where interference effects are significant is discussed. Section IV contains close-coupling results for elastic scattering cross sections. All results have been obtained by solving coupled equations involving only open channels.

II. VERIFICATION OF CALCULATION METHOD

The calculations were carried out using the cou-

pled radial Schrödinger equations in the total-angular-momentum representation.[5] These equations were solved by the integral-equation method of Sams and Kouri[6] to yield the scattering T-matrix elements. Then the expressions for the differential and total cross sections developed by Blatt and Biedenharn[7] were employed to sum the various products of T elements so as to satisfy the proper boundary conditions. In this study, two forms of the equation for the differential cross sections derived by Blatt and Biedenharn[7] were examined. If the cross section $\sigma(\theta)$ is expressed in the following series of Legendre polynomials,

$$\frac{d\sigma_{j'j}}{d\theta} = [K_j^2(2j+1)]^{-1} \sum_{\lambda=0}^{\infty} B_\lambda(j' \mid j) P_\lambda(\cos\theta) ,$$

then the B_λ is given by either

$$B_\lambda(j' \mid j) = (-1)^{j'-j} \tfrac{1}{4} \sum_{J_1} \sum_{J_2} \sum_{l_1} \sum_{l_2} \sum_{l_1'} \sum_{l_2'} Z(l_1 J_1 l_2 J_2;\, j\lambda)\, Z(l_1' J_1 l_2' J_2;\, j'\lambda) \mathrm{Re}[T^{J_1}(j'l_1';\, jl_1)^* T^{J_2}(j'l_2';\, jl_2)] \tag{1}$$

or

$$B_\lambda(j' \mid j) = (-1)^{j'-j} \frac{1}{4} \sum_{J=0}^{\infty} \sum_{l=|J-j|}^{J+j} \sum_{l'=|J-j'|}^{J+j'} Z(lJlJ;\, j\lambda) Z(l'Jl'J;\, j'\lambda) \left| T^J(j'l';\, jl) \right|^2$$

$$+ \frac{(-1)^{j'-j}}{2} \sum_{J_1=0}^{\infty} \sum_{l_1=|J_1-j|}^{J_1+j} \sum_{l_1'=|J_1-j'|}^{J_1+j'} \left(\sum_{J_2=J_1+1}^{\infty} \sum_{l_2=|J_2-j|}^{J_2+j} \sum_{l_2'=|J_2-j'|}^{J_2+j'} Z(l_1 J_1 l_2 J_2;\, j\lambda) Z(l_1' J_1 l_2' J_2;\, j'\lambda) \right.$$

$$\times \mathrm{Re}[T^{J_1}(j'l_1';\, jl_1) T^{J_2}(j'l_2';\, jl_2)] + \sum_{l_2=l_1+1}^{J_1+j} \sum_{l_2'=|J_1-j'|}^{J_1+j'} Z(l_1 J_1 l_2 J_1;\, j\lambda) Z(l_1' J_1 l_2' J_1;\, j'\lambda)$$

$$\times \mathrm{Re}[T^{J_1}(j'l_1';\, jl_1) T^{J_1}(j'l_2';\, jl_2)]$$

$$\left. + \sum_{l_2'=l_1'+1}^{J_1+j'} Z(l_1 J_1 l_1 J_1;\, j\lambda)\, Z(l_1' J_1 l_2' J_1;\, j'\lambda)\, \mathrm{Re}[T^{J_1}(j'l_1';\, jl_1) T^{J_1}(j'l_2';\, jl_1)] \right) . \tag{2}$$

The quantities Z are well-known combinations of vector coupling coefficients and are given by Blatt and Biedenharn[7] in terms of the 6-j symbols. The first expression involves a number of redundant terms since the symmetry properties of the Raccah coefficients and the T-matrix elements have not been utilized, while the second expression does not involve such terms.[7,8] It was found that use of the second form along with selection rules (triangle inequalities) and Raccah's expression for the 6-j symbols, provided considerable savings in computation time. To test our programs, calculations for the He-H_2 collision system were carried out for comparison with the study of this system by Johnson and Secrest.[9] In Table I, the values of B_λ obtained by Johnson and Secrest are compared with the present results. Both have been computed using a total of 15 values of the total-angular-momentum quantum number $J(J_{max}=14)$. All possible B_λ values have been calculated for this value of J_{max}. In Fig. 1, $\sigma(\theta)$ is plotted using λ_{max} equal to 3 and 28. Although both give strong backward peaking in the scattering, it appears that some care must be exercised to assure that convergence in the sum over λ is attained for all values of θ. If one compares the B_λ values in Table I, it appears clear that the B_λ for λ ranging from 4 to 16 can also contribute to the differential cross section since cumulatively they can make a contribution to the fourth decimal. In the backward scattering region, these are clearly unimportant. However, in the forward direction, and especially when θ is zero, their contribution is

TABLE I. $B_\lambda(j';j)$ values for the $j=0$ to $j'=2$ transition in He-H_2 collisions.

Johnson-Secrest results[a]	Present results
$B_0(2;0) = 0.0241$	$B_0(2;0) = 0.024\,26$
$B_1(2;0) = -0.0281$	$B_1(2;0) = -0.028\,17$
$B_2(2;0) = 0.0048$	$B_2(2;0) = 0.004\,83$
$B_3(2;0) = 0.0006$	$B_3(2;0) = 0.000\,57$
	$B_4(2;0) = 0.000\,24$
	$B_5(2;0) = 0.000\,16$
	$B_6(2;0) = 0.000\,11$
	$B_7(2;0) = 0.000\,02$
	$B_8(2;0) = 0.000\,08$
	$B_9(2;0) = 0.000\,14$
	$B_{10}(2;0) = 0.000\,13$
	$B_{11}(2;0) = 0.000\,08$
	$B_{12}(2;0) = 0.000\,01$
	$B_{13}(2;0) = -0.000\,02$
	$B_{14}(2;0) = -0.000\,03$
	$B_{15}(2;0) = -0.000\,01$
	$B_{16}(2;0) = -0.000\,01$

[a] They report values for $\lambda_{max}=3$ only. The same values for J_{max} are used in both their calculations and those reported here.

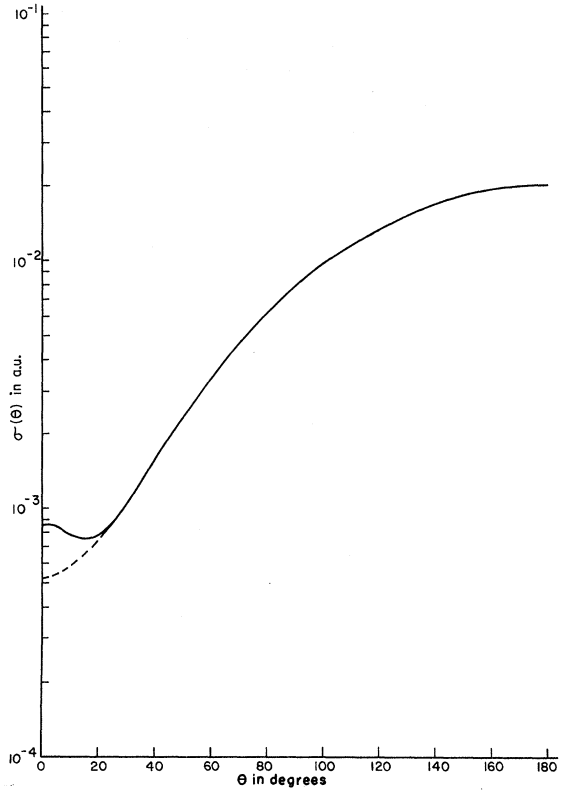

FIG. 1. $j=0$ to $j=2$ inelastic differential scattering cross section for He-H_2 collisions. The solid curve is computed using $\lambda_{max}=28$ and the dashed curve using $\lambda_{max}=3$.

quite significant since $\sigma(\theta)$ is the sum of the B_λ [note $P_\lambda(1)=1$ for all λ]. This effect is clearly shown in Fig. 1 in the enhancement of the forward scattering when B_λ through $\lambda=28$ are included compared to when only B_λ through B_3 are included. The convergence on λ is also important for the H-H_2 results which are discussed in Sec. III.

The total cross section σ may be written as

$$\sigma=\sum_l(2l+1)A_l\,, \tag{3}$$

where A_l may be interpreted as a relative probability for excitation due to that particular l wave.[1] Table II and Fig. 2 contain the values and a plot,

TABLE II. Relative probabilities for the $0\rightarrow 2$ excitation in He-H_2 scattering.

$A_0=0.625\times10^{-3}$	$A_6=0.150\times10^{-3}$
$A_1=0.579\times10^{-3}$	$A_7=0.75\times10^{-4}$
$A_2=0.520\times10^{-3}$	$A_8=0.26\times10^{-4}$
$A_3=0.432\times10^{-3}$	$A_9=0.6\times10^{-5}$
$A_4=0.337\times10^{-3}$	
$A_5=0.241\times10^{-3}$	

$\sigma_{tot}(2\leftarrow0)=0.0173$; Johnson-Secrest $\sigma_{tot}(2\leftarrow0)=0.0173$ in molecular units.

respectively, of the A_l which are the partial-wave contributions to the total cross sections σ. It is clear that these relative probabilities favor excitation by head-on collisions and one expects such collisions to contribute significant backward scattering. This conclusion is borne out by the differential cross section shown in Fig. 1.

III. CLOSE-COUPLING RESULTS FOR $j=0$ TO $j=2$ TRANSITIONS IN H-H_2 COLLISIONS

In order to facilitate a detailed comparison of the close-coupled results for rotational excitation in low-energy H-H_2 collisions with the distorted-wave calculations of Tang, the potential function reported by Tang[1] has been used in all of the close-coupled calculations reported here. When this is done, it is found that the close-coupled results agree with the qualitative features of the distorted-wave results for the differential cross sections and the relative probabilities A_l for collision energies $E=0.1$, 0.15, and 0.25 eV. In addition, the total cross sections are in excellent quantitative agreement with those of Tang. There are some differ-

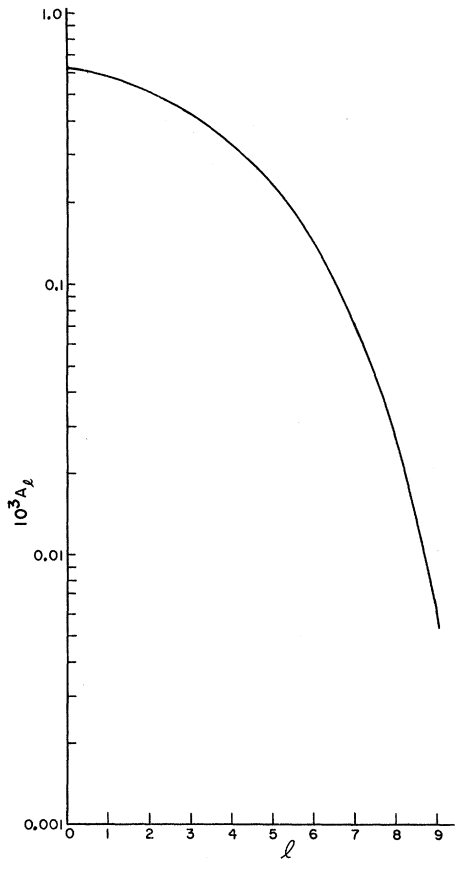

FIG. 2. Relative inelastic $j=0$ to $j=2$ probabilities A_l for He-H_2 collisions.

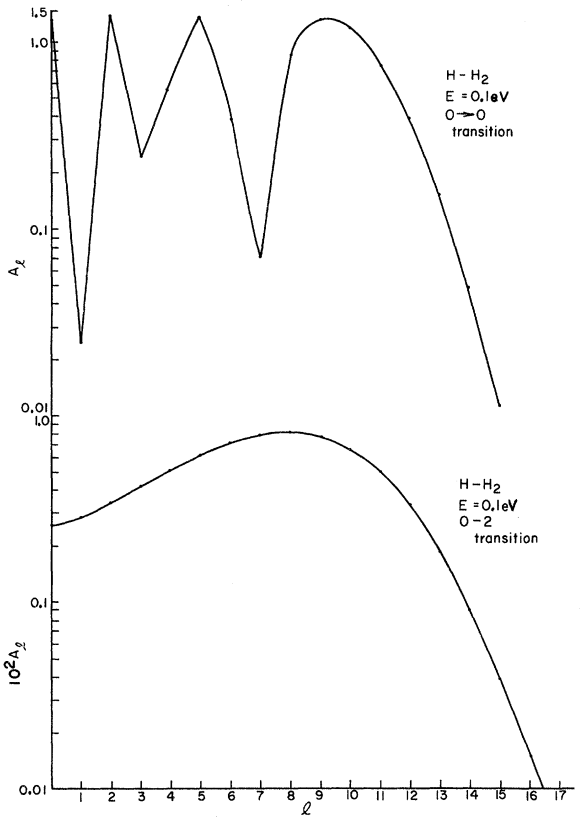

FIG. 3. Relative probabilities A_l for H-H_2 collisions at $E = 0.1$ eV. The upper curve gives A_l for $j = 0$ elastic scattering and the lower curve gives A_l for $j = 0$ to $j = 2$ inelastic scattering.

ences between the close-coupling and distorted-wave results. However, the over-all agreement between the two is actually very encouraging. This is of particular interest in connection with the interpretation of the differential cross sections by Tang in terms of the relative importance of various partial waves and whether they contribute to forward or backward scattering.

With this in mind, we have the relative probabilities A_l for excitation plotted in the lower portions of Figs. 3–5. As in the case of Tang's results, at energies 0.1 and 0.15 eV, a single peak occurs for $l \neq 0$. However, in both cases, the exact position of the maximum A_l differs from Tang's. Additionally, even though the close-coupled results for the total cross section σ_{tot}^{cc} and Tang's result σ_{tot}^{Tang} are essentially the same,[10] the curves of the close-coupled values of A_l are much flatter than Tang's and the maximum A_l is smaller than his. In spite of these differences in the A_l curves, the total cross sections agree quite well quantitatively. This is apparently due in part to the compensating effect of the weight factor $(2l+1)$ which appears in Eq. (3). In the case of $E = 0.25$ eV, again there is qualitative agreement with Tang in the appearance of two maxima in the A_l plot. As in the case of the lower energies, the exact positions of the maxima are slightly shifted. However, in the close-coupled calculations, the large-l maximum is lower than the $l = 0$ maximum. This is just the reverse of results obtained by the distorted-wave method at 0.25 eV. Moreover, both the 0.1- and 0.15-eV close-coupling maxima were lower than the distorted-wave results (although at 0.15 eV the close-coupled results are closer to the distorted-wave results than at 0.1 eV). However, at 0.25 eV, the $l = 0$ close-coupling maximum is larger than the $l = 0$ distorted-wave maximum while the higher-l close-coupling maximum is again lower. It is possible that these slight differences are more strongly manifest in the angular distributions for the inelastic scattering. Indeed, the presence of a broader peak in the A_l plots and the differences in the l values at which peaking occurs would be expected to change the angular distribution primarily by changing the angles θ at which oscillations occur. However, one would not expect a significant change in the over-all shape of the $\sigma(\theta)$ curves, so that one still should see strong forward

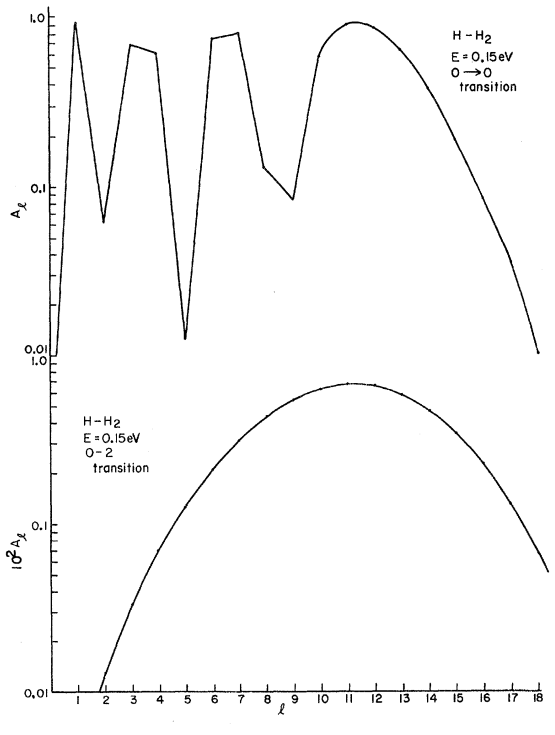

FIG. 4. Relative probabilities A_l for H-H_2 collisions at $E = 0.15$ eV. The upper curve gives A_l for $j = 0$ elastic scattering and the lower curve gives A_l for $j = 0$ to $j = 2$ inelastic scattering.

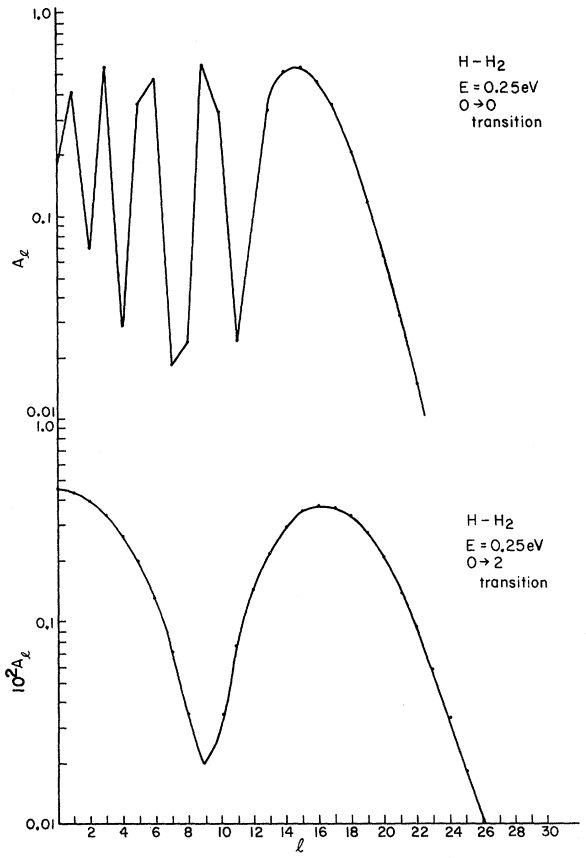

FIG. 5. Relative probabilities A_l for H-H_2 collisions at $E = 0.25$ eV. The upper curve gives A_l for $j = 0$ elastic scattering and the lower curve gives A_l for $j = 0$ to $j = 2$ inelastic scattering.

peaking in the 0.1- and 0.15-eV cross sections and the beginning of backward peaking in the 0.25-eV scattering due to the presence of the $l = 0$ peak in the A_l.

Figures 6—11 contain plots of the differential cross sections $\sigma(\theta)$ for the close-coupling and distorted-wave calculations. It is immediately noted that the qualitative features are the same except for the beginning of a small backscattering peak in the close-coupling results at $E = 0.15$ eV. Otherwise, the close-coupling results at 0.1 and 0.15 are characterized by strong forward peaking, and the 0.25-eV results show strong forward peaking along with the significant growth of a backward peak. Close inspection of the plots also shows that the present close-coupling results are substantially larger than Tang's distorted-wave results.[11] In addition, the positions of the oscillations in the forward scattering region differ. It is likely that these differences are real and not the result of not including enough B_λ values in obtaining the distorted-wave results. This conjecture is supported by the fact that the close-coupling results at $E = 0.1$ eV and $\lambda_{max} = 34$ and 60 are extremely close to one another for all θ; at $E = 0.15$ eV, the close-coupling results for λ_{max} equal to 38 and 60 are qualitatively the same for angles less than around 30°; at $E = 0.25$ eV, the close-coupling results are qualitatively the same for λ_{max} equal to 58 and 70 and angles less than 80°. Even at 0.15 and 0.25 eV, the differences in the forward direction are much smaller in magnitude than the corresponding differences in the distorted-wave and close-coupling results. At the energies 0.15 and 0.25 eV, one also has important qualitative differences for larger-angle scattering. Thus, the close-coupling results at $E = 0.15$ eV have a backscattering component that does not appear in the distorted-wave results. Also, more oscillations in the smaller-angle scattering occur in Tang's results. However, it is difficult to say whether these additional oscillations are a result of the distorted-wave approximation or a failure to include enough B_λ values in computing $\sigma(\theta)$. It should be noted that similar spurious oscillations arise in the close-coupling results if one sums only up to $\lambda = 58$ and they dis-

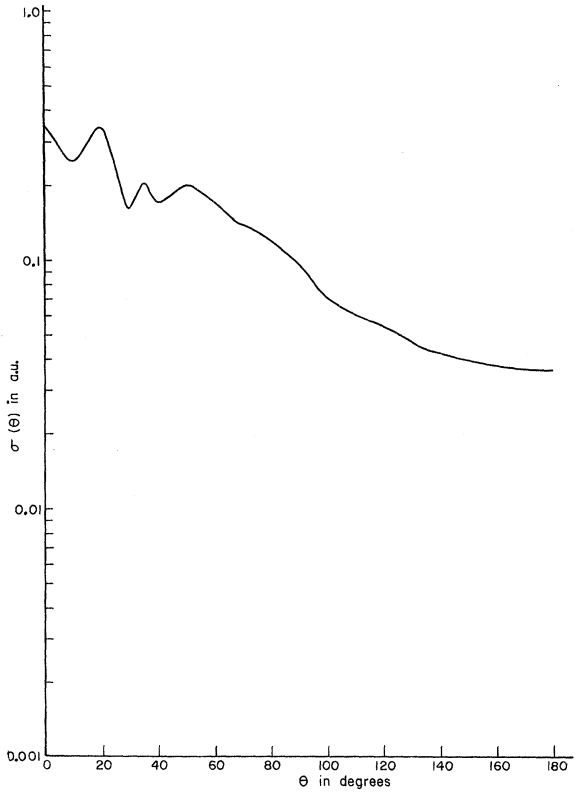

FIG. 6. Tang's distorted-wave differential cross section for the $j = 0$ to $j = 2$ transition at $E = 0.1$ eV.

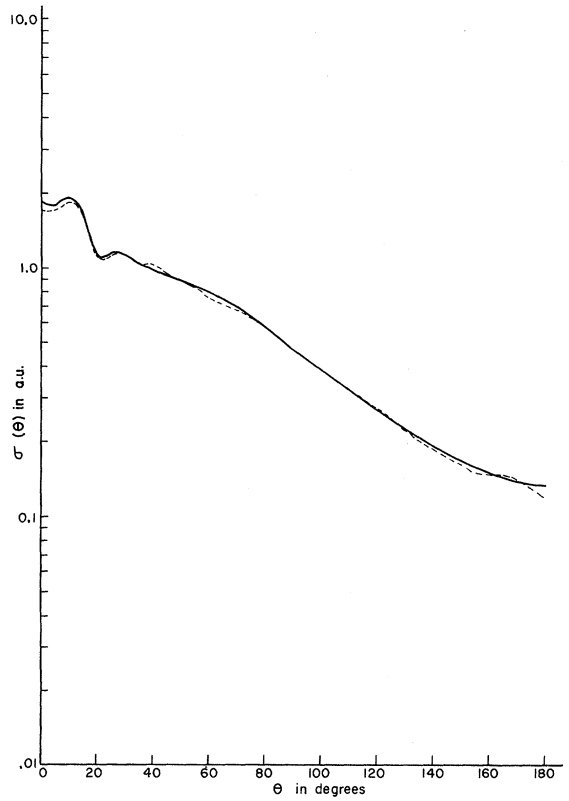

FIG. 7. Close-coupling differential cross section for the $j=0$ to $j=2$ transition at $E=0.1$ eV. The solid curve is for $\lambda_{max}=34$.

appear when B_λ up to B_{70} are included. At $E=0.25$ eV, the positions and number of oscillations differ in the close-coupling and the distorted-wave results. It appears that the small-angle differences are real, but whether the differences at larger angles are due to the distorted-wave approximation or to insufficient number of B_λ is not clear. These results point up the importance of making sure that convergence in the expansion of $\sigma(\theta)$ is obtained. It is also to be noted that convergence in one region of angles will not necessarily imply convergence over the entire range of θ since interference effects may cause the B_λ for large λ to dominate over certain intervals. In the close-coupling calculations, it is felt that reasonable convergence in computing the $\sigma(\theta)$ has been obtained in the calculations where $\lambda_{max}=60$ for $E=0.1$ and 0.15 eV, and $\lambda_{max}=70$ for $E=0.25$ eV (see Figs. 6–11).

IV. CLOSE-COUPLING RESULTS FOR ELASTIC $j=0$ TO $j=0$ SCATTERING IN H-H_2 COLLISIONS

The elastic scattering for $j=0$ to $j=0$ is of particular interest since it complements the inelastic scattering data because the spherically symmetric term $V_0(R)$ in the potential dominates the elastic scattering, whereas $V_2(R)$ dominates the inelastic processes.[12] Thus, the two multipole components of $V(R)$ may be studied more or less independently. In obtaining these close-coupled results, the convergence of the elastic cross section with respect to the number of B_λ values included in the computation was investigated in some detail. For the three energies considered here, it appears to be necessary to include B_λ values that are three orders of magnitude smaller than the largest B_λ value.

The qualitative features of the differential cross sections may again be interpreted using the relative probabilities A_l for the various partial waves. If one considers the upper portions of Figures 3–5 compared with the lower portions of the figures, one is struck by the rapid oscillations in the values of the A_l for elastic scattering at all three energies compared to the smooth variation in the A_l for inelastic scattering. This behavior is readily understood if one makes the assumption that the effects

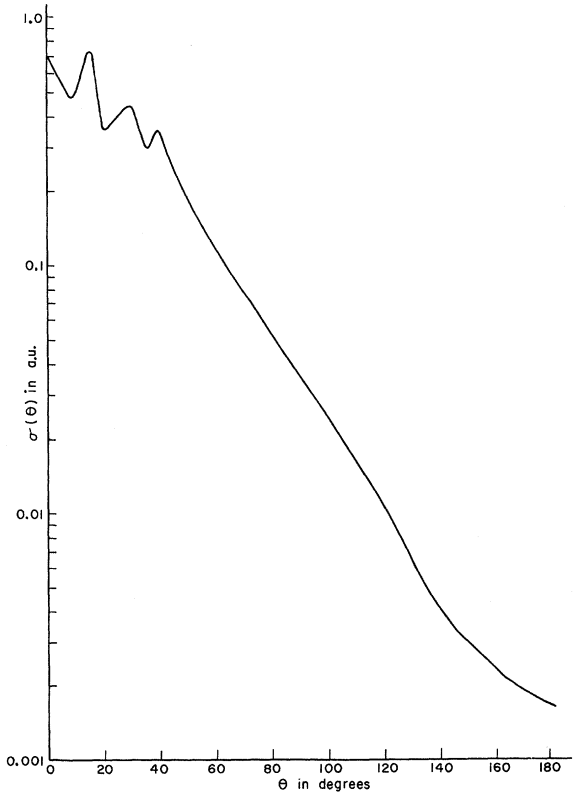

FIG. 8. Tang's distorted-wave differential cross section for the $j=0$ to $j=2$ transition at $E=0.15$ eV.

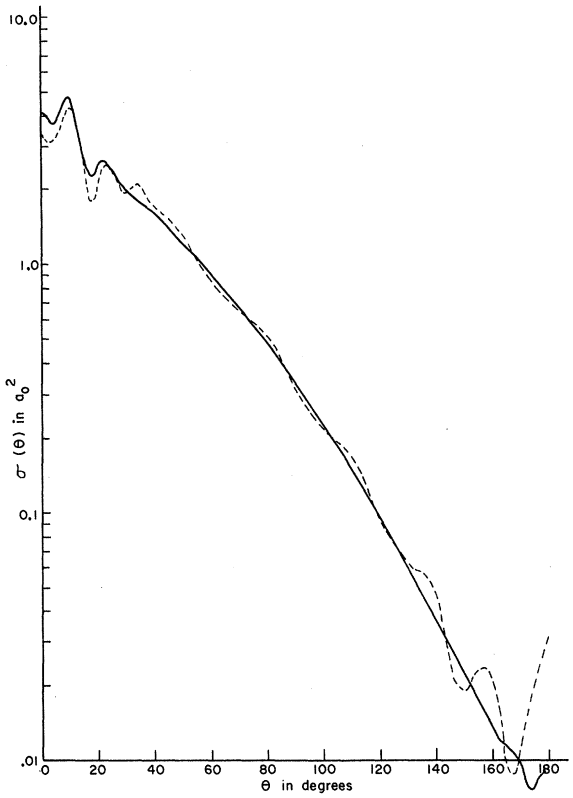

FIG. 9. Close-coupling differential cross section for the $j=0$ to $j=2$ transition at $E=0.15$ eV. The solid curve is for $\lambda_{max}=60$ and the dashed curve is for $\lambda_{max}=38$.

of backcoupling are relatively negligible for the elastic scattering.[13] Then one may write

$$\sigma_{tot}=(4\pi/k^2)\sum_l(2l+1)\sin^2\delta_l \tag{4}$$

or

$$A_l=(4\pi/k^2)\sin^2\delta_l \tag{5}$$

for the elastic scattering A_l. (This, of course, is equivalent to saying the T matrix is approximately diagonal.) Consideration of the spherical multipole term $V_0(R)$ shows that it has both a well and a repulsive core. However, the well is quite shallow and it occurs at a fairly large R value. To the degree that $V_0(R)$ can be considered as monotonic, one has that δ_l, the lth phase shift, must be negative. (The presence of the well will cause the true phase shift to have "wiggles" as a function of l.) The A_l will have oscillations characteristic of $\sin^2\delta_l$ which produces the observed behavior[13] in Figs. 3–5.

Considering $\sigma(\theta)$ (see Figs. 12–14), at an energy of 0.1 eV one has a substantial value for A_0 and as a result $\sigma(\theta)$ has a slight upturning at 180°. For an energy of 0.15 eV, A_0 is small compared to A_l for higher l values. Therefore one anticipates no significant backscattering as is borne out by the close-coupling results. At an energy of 0.25 eV, A_0 is again comparable to some of the A_l for larger l's and one again finds a behavior similar to that at 0.1 eV.

These considerations are offered as a preliminary interpretation. More detailed calculations of the elastic scattering using both coupled equations and also just the uncoupled $j=0$ equation are planned in order to test these ideas. In addition, further calculations are needed to test the degree of convergence of the Legendre expansion for elastic scattering. The possible influence of the $V_2(R)\times P_2(\cos\theta)$ term on elastic scattering can be studied by the uncoupled calculations (using only $j=0$) mentioned above. Finally, if the potential well will support bound states, then the possible importance of single-particle resonances and virtual excitation resonances for elastic and inelastic scattering will be examined.

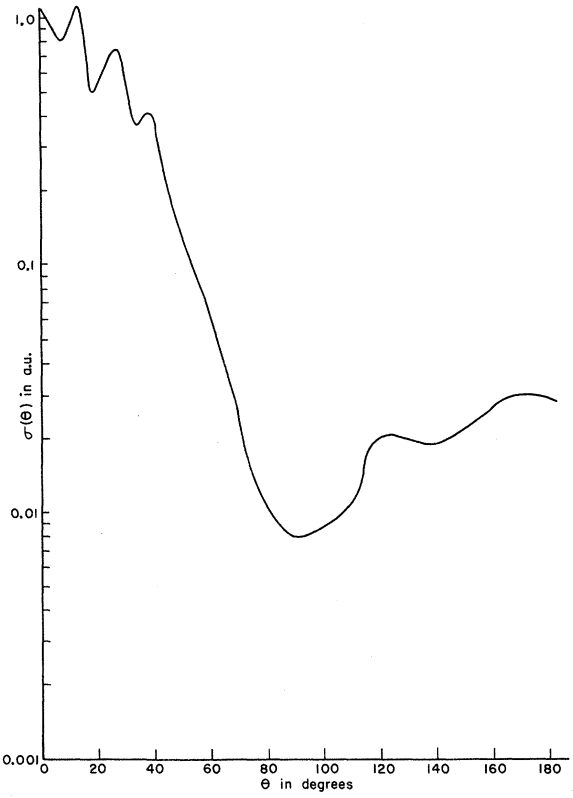

FIG. 10. Tang's distorted-wave differential cross section for the $j=0$ to $j=2$ transition at $E=0.25$ eV.

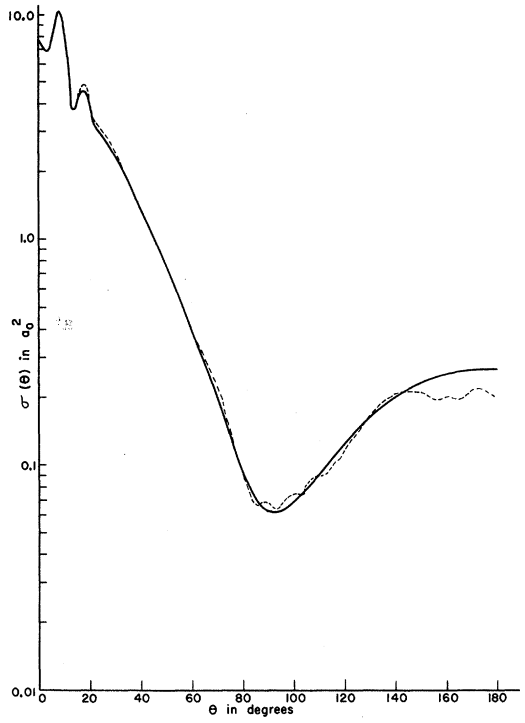

FIG. 11. Close-coupling differential cross section for the $j=0$ to $j=2$ transition at $E=0.25$ eV. The solid curve is for $\lambda_{max}=70$ and the dashed curve is for $\lambda_{max}=58$.

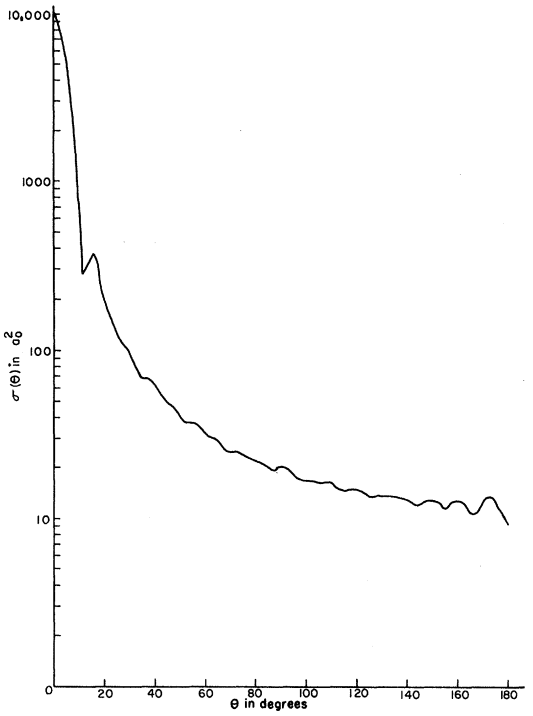

FIG. .13. Close-coupling differential cross section for $j=0$ elastic scattering at $E=0.15$ eV and $\lambda_{max}=60$.

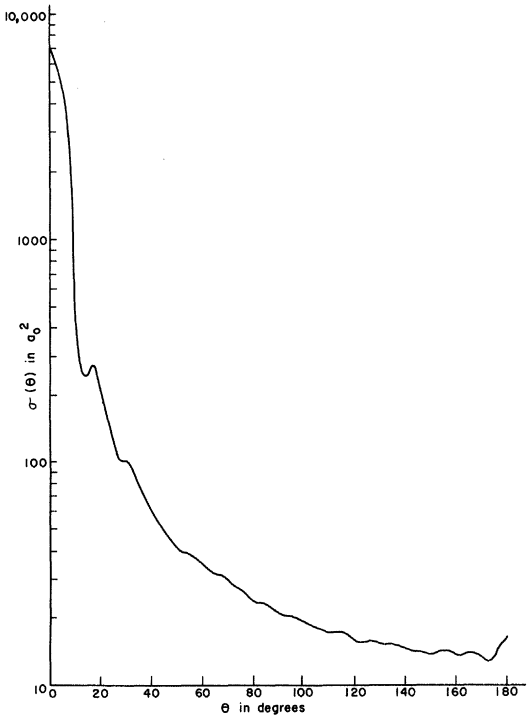

FIG. 12. Close-coupling differential cross section for $j=0$ elastic scattering at $E=0.1$ eV and $\lambda_{max}=60$.

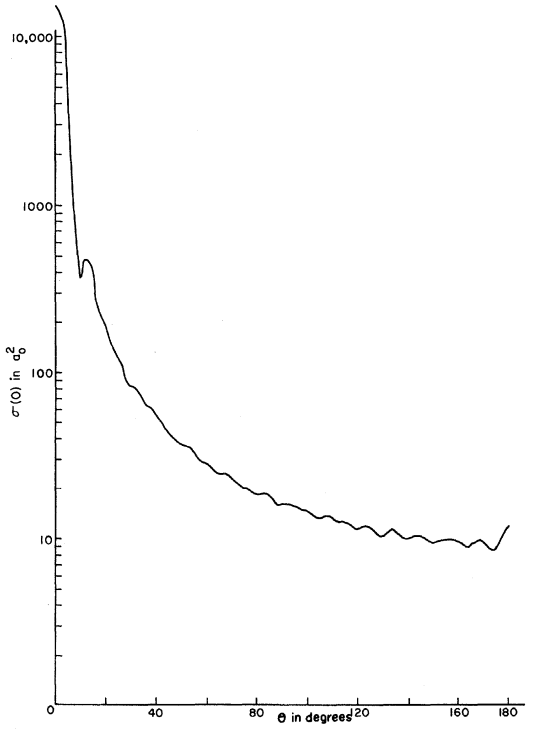

FIG. 14. Close-coupling differential cross section for $j=0$ elastic scattering at 0.25 eV and $\lambda_{max}=70$.

ACKNOWLEDGMENTS

The authors express their appreciation to Professor Neal F. Lane for providing programs which were used in developing the differential cross-section routines used in the present investigation. Helpful comments by Professor K. T. Tang are gratefully acknowledged. This work was supported in part by grants to the University of Houston and Rice University from the National Science Foundation. One of the authors (D. J. K.) gratefully acknowledges Lockheed Electronics Company and Dr. Bryan Oldham, Dr. Andrew Potter, and Dr. Ben Carroll for their support during the time this research was initiated.

[1]K. T. Tang, Phys. Rev. 187, 122 (1969).

[2]K. T. Tang and M. Karplus, J. Chem. Phys. 49, 1676 (1968).

[3]A. Dalgarno, R. J. W. Henry, and C. S. Roberts, Proc. Phys. Soc. (London) 88, 611 (1966).

[4]A. C. Allison and A. Dalgarno, Proc. Phys. Soc. (London) 90, 609 (1967).

[5]A. M. Arthurs and A. Dalgarno, Proc. Phys. Soc. (London) A256, 540 (1960).

[6]W. N. Sams and D. J. Kouri, J. Chem. Phys. 51, 4809 (1969); 51, 4815 (1969).

[7]J. M. Blatt and L. C. Biedenharn, Rev. Mod. Phys. 24, 258 (1952).

[8]G. Racah, Phys. Rev. 61, 186 (1942); 62, 438 (1942); 63, 367 (1943). Also, L. C. Biedenharn, J. M. Blatt, and M. E. Rose, Rev. Mod. Phys. 24, 249 (1952).

[9]B. R. Johnson and D. Secrest, J. Chem. Phys. 48, 4682 (1968).

[10]The precise values of $\sigma_{\text{tot}}^{\text{cc}}$ are 1.107 bohr^2 at $E=0.1$ eV, 1.278 bohr^2 at $E=0.15$ eV, and 1.183 bohr^2 at $E=0.25$ eV.

[11]There does not appear to be a constant scale factor which would bring the distorted-wave and close-coupling results for $\sigma(\theta)$ into agreement for all values of θ. Further, agreement of $\sigma_{\text{tot}}^{\text{cc}}$ and $\sigma_{\text{tot}}^{\text{Tang}}$ requires only agreement of the B_0 coefficient, while the B_λ for $\lambda \neq 0$ may still differ significantly.

[12]If the potential is expressed in the multipole form $V(\vec{R}) = V_0(R) + V_2(R)P_2(\cos\theta)$, then for the $j=0$ elastic scattering, the matrix element of $P_2(\cos\theta)$ is zero so the "adiabatic" potential is simply $V_0(R)$. The $V_2(R)P_2(\cos\theta)$ term affects the $j=0$ elastic scattering only by causing excitations to and from the $j=2$ rotator state.

[13]W. H. Miller (private communication).

PHYSICAL REVIEW A VOLUME 4, NUMBER 3 SEPTEMBER 1971

Low-Energy Electron Ejection of Atoms in Collisions with Relativistic Electrons

J. N. Das

Nabadwip Vidyasagar College, Nadia, West Bengal, India

(Received 15 May 1970; revised manuscript received 9 November 1970)

Low-energy electron-ejection cross sections of atoms in collisions with relativistic electrons have been calculated. The calculations are similar to those of Weber *et al.* In the approximate integration of the differential cross section over certain angles, Weber *et al.* considered Z small and obtained a $(\alpha Z)^4$-dependent result. We have followed a different type of approximation, valid for $Z \gg 1$, and obtained the explicit $(\alpha Z)^5$-dependent result. The result shows a much stronger dominance of the distribution of ejected electrons over the "Parzen distribution" in the low-energy region than the results of Weber *et al.* when applied to atoms with $Z \gg 1$.

I. INTRODUCTION

Mullin and co-workers have pointed out[1,2] that the low-energy large-angle scattering of electrons from atomic bound electrons in collisions with relativistic electrons may be sufficient to mask the "Parzen peak" that exists in the low-energy region of scattered electrons which have lost energy in the bremsstrahlung production. For high-energy colliding electrons, the Parzen peak[3] is situated at an energy W of the scattered electrons for which $1 < W \lesssim 1.2\ mc^2$ (or in terms of momentum, $0 < p \lesssim \frac{2}{3} mc$). The "Parzen distribution" is, moreover, independent of the nuclear charge Z of the atoms.

Weber *et al.*, in Ref. 2, have given a relativistic treatment to the scattering of low-energy electrons by bound electrons. In that paper they have described the bound and ejected electrons with wave functions which are obtained by an expansion in the parameters αZ and $\alpha Z/\beta$, and which are correct to first relative orders in these expansion parameters. Consistent with the neglect of higher powers of $\alpha Z/\beta$ in the wave functions, Weber *et al.* have a cross section which is valid to the lowest order in $(\alpha Z)^5$ and the highest order in the energy W_i of the incident electron. In the approximate evaluation of certain integrals[4] I_{nm} occurring in the expression for the cross section, they considered